

## Dielectric and conducting behavior of pyrene functionalized PANI/P(VDF-co-HFP) blend

Veer Pal Singh,<sup>1</sup> Ramasubbu Ramani,<sup>1</sup> Ajit Shankar Singh,<sup>1</sup> Preeti Mishra,<sup>1</sup> Vijay Pal,<sup>1</sup> Amit Saraiya<sup>2</sup>

<sup>1</sup>Polymer Science Division, DMSRDE, G.T. Road, Kanpur 208 013, India

<sup>2</sup>Nanoscience Technology Division, DMSRDE, G.T. Road, Kanpur 208 013, India

Correspondence to: R. Ramani (E-mail: ramanir70@rediffmail.com)

**ABSTRACT:** Herein, we present the dielectric and electrical conductivity properties of the partially miscible polymer blend prepared using pyrene functionalized polyaniline (pf-PANI) and poly(vinylidene fluoride-co-hexafluoro propylene) (PVDF-co-HFP). The blend mostly retains the fluorescent nature of pf-PANI as well as can be moldable and possesses good damping property. The dielectric properties have been investigated as a function of temperature at three different frequencies and the plausible origin of polarization responsible for dielectric behavior in this blend has been identified. The experimental results of dielectric measurements are compared with theoretical models and discussed. The surface morphology of the samples has been examined with a scanning electron microscope. The electrical conductivity has also been studied as a function of temperature and explained in terms of hopping of charge carriers/interconnected networks. The combined dielectric and conductivity results together with scanning electron microscope micrographs, reveal that there is hindrance to achieve percolation threshold even after pf-PANI addition of 57 vol % and subsequent thermal treatment. © 2016 Wiley Periodicals, Inc. *J. Appl. Polym. Sci.* **2016**, *133*, 44077.

**KEYWORDS:** blends; conducting polymers; copolymers; dielectric properties; structure-property relations

Received 15 February 2016; accepted 9 June 2016

DOI: 10.1002/app.44077

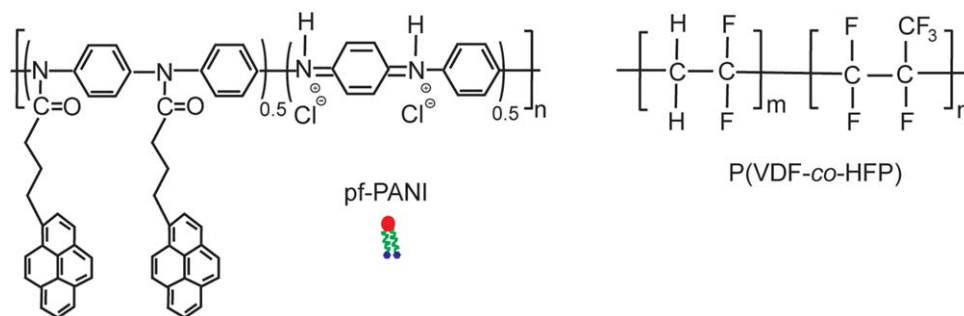
### INTRODUCTION

The dielectric constant ( $\epsilon'$ ) of common polymers is very low ( $<10$ ) and researchers have demonstrated that incorporating ceramics into polymers can efficiently improve its dielectric constant.<sup>1–3</sup> However, high loading of ceramics (usually over 50 vol %) dramatically decreases the mechanical properties of polymers.<sup>3,4</sup> In the recent past, polymer/conductive filler dielectric (PCD) materials are preferred over other ceramic based systems as they are flexible and moldable.<sup>3,5</sup> In a conventional PCD material, the distance between the fillers can usually be controlled by filler loading. The existence of insulator polymer layers between conductive particles serves as electrical barriers and impairs direct contact between them. If the distance between the conductive fillers becomes small enough to permit tunneling effect, this could lead to leakage current and subsequent conduction. This optimum filler level is called the percolation threshold, above which a significant increase in dielectric constant together with a large undesirable increase in dissipation factor ( $\tan \delta$ ) value, usually by 1 order of magnitude or more is observed.<sup>3,6,7</sup> Thus, the dielectric constant, dielectric loss, and conductivity all expected to show an abrupt change near the percolation threshold in an insulator-conductor system.<sup>3</sup>

If the conductive filler happens to be a conducting polymer, it has an added advantage that the modulus of the resulting material will not change very much from that of the insulating polymer matrix<sup>6,8,9</sup> but will have much higher mechanical characteristics compared with conducting polymer that is used as filler.<sup>10–12</sup> The origin of high dielectric constant at the percolation threshold in an all polymer insulator-conductor system is generally explained by a combination of microcapacitance structure model and the interfacial polarization<sup>6,13,14</sup> and the electrical conductivity by the hopping of the charges and the interconnected network leading to a conductive path.<sup>15,16</sup>

Amongst conducting polymers, polyaniline (PANI) is a very promising candidate since the monomer aniline is of low cost and it possesses multifunctional applications.<sup>17,18</sup> The synthetic PANI is brittle in nature, mechanically weak, and hence can be used as conductive/dielectric filler in an insulating polymer matrix.<sup>18</sup> In the past, PANI has been used as filler in polymers like poly(vinyl alcohol),<sup>19,20</sup> polyurethane,<sup>21</sup> epoxy,<sup>22</sup> and ethylene vinyl acetate (EVA)<sup>23</sup> and have resulted to change in dielectric and/or conducting properties.

In the recent years, electroactive polymers such as poly(vinylidene fluoride) (PVDF) and its copolymers draw considerable attention owing to their application in high efficiency charge



**Scheme 1.** Chemical formulas of pyrene functionalized polyaniline (pf-PANI) and poly(vinylidene fluoride-co-hexafluoro propylene) P(VDF-co-HFP) are schematically shown. [Color figure can be viewed in the online issue, which is available at [wileyonlinelibrary.com](http://wileyonlinelibrary.com).]

storage capacitors.<sup>24</sup> This is because, the PVDF-based polymers have the highest dielectric constant amongst polymers.<sup>25</sup> The incorporation of amorphous phase of hexafluoropropylene (HFP) into the main constituent vinylidene fluoride (VDF) blocks was reported to modify some of the properties of the homopolymer.<sup>25,26</sup> Particularly, the degree of crystallinity in poly(vinylidene fluoride-co-hexafluoro propylene) [P(VDF-co-HFP)] is significantly reduced in comparison with PVDF, while the flexibility and solubility in organic solvents are enormously increased.<sup>25,26</sup>

Interesting dielectric and/or conductivity studies on PANI/PVDF based materials have been reported.<sup>4,6,8,9,11,12,14,16,27–29</sup> The first high dielectric all-polymer material using PANI as conducting polymer particulates in the PVDF-based terpolymer poly(vinylidene fluoride-co-trifluoroethylene-co-chloro trifluoroethylene) [P(VDF-TrFE-CTFE)] has been reported more than a decade back.<sup>27</sup> In case of PCD systems based on PANI/PVDF as well as PANI/PVDF copolymers, percolative threshold with 13 to 30 vol % of PANI content have been reported.<sup>8,9,12,29</sup> Interestingly, few other studies report that using even lower content of PANI (<5 vol %) as conductive filler and PVDF as an insulating matrix, enhancement in dielectric constant and  $\tan \delta$  were observed.<sup>6,16</sup> It is also possible that heat treatment can bring the particles close to one another to form a conductive network.<sup>16</sup>

Despite of good dielectric and conductivity properties of PANI/PVDF system, PANI is not compatible with PVDF and its copolymers.<sup>30,31</sup> But, when functionalized protonic acids like DBSA are used as doping agents in PANI chains, it can form compatible blends with PVDF.<sup>30</sup> Recently, PANI doped with DBSA has been blended with P(VDF-co-HFP) and improvement in the processibility of the copolymer has been reported.<sup>14</sup> We have reported the preparation and properties of the first polymer blend using the pyrene functionalized PANI (pf-PANI).<sup>31</sup> In this work, pf-PANI was blended with P(VDF-co-HFP) in equal weight ratio. The synthesized pf-PANI was fluorescent and brittle. But, upon blending it with P(VDF-co-HFP), it became flexible and developed good damping ability without significant loss in its fluorescent property, at least in its solution phase.<sup>31</sup>

Herein, we have made an attempt to understand the dielectric and conductive behavior of pf-PANI/P(VDF-co-HFP) blend in which pf-PANI is used as a conductive/dielectric filler and P(VDF-co-HFP) as the insulating matrix. Incidentally, in this equal weight ratio of pf-PANI/P(VDF-co-HFP) blend, the content of pf-PANI turns out to be 57 vol % which is much higher

than the percolation threshold of PANI content reported for PANI/PVDF-based percolating systems.<sup>8,9,12,29</sup> The study has also been extended to understand whether thermal treatment could bring the pf-PANI particles to close proximity and can cause percolation threshold-like change in dielectric and conducting behavior of this blend.

## EXPERIMENTAL

### Sample Preparation

Pellets of copolymer of vinylidene fluoride and hexafluoro propylene P(VDF-co-HFP) having  $M_w = 400,000$  g/mol and  $M_n = 130,000$  g/mol used in this study, was obtained from Sigma-Aldrich. This copolymer is named here as PVH. The PVH was dried in vacuum at 50 °C for 24 h before use. All the chemicals used in this study were also obtained from Sigma-Aldrich.

The detailed procedure for the synthesis of pf-PANI and pf-PANI/PVH blend can be found from our earlier work.<sup>31</sup> In brevity, the pf-PANI/PVH blend was prepared by mixing pf-PANI and PVH in *N*-methyl-2-pyrrolidone (NMP) solvent (1 wt % solution) so as to form a blend with equal weight ratio. The mixing was continued for 24 h and the solvent was gradually evaporated thoroughly in air under a fume-hood for 48 h and then kept in vacuum oven at 50 °C for 1 week, which results to smooth film formation. The chemical structure of the pf-PANI and P(VDF-co-HFP) polymers are shown in Scheme 1.

### Characterization

**Dielectric Measurements.** The dielectric measurements were conducted in the temperature range of  $-100$  to  $100$  °C with a heating rate of  $2$  °C at three different frequencies 1, 10, and 100 kHz using DS 6000 Dielectric Analyzer of M/s. Lacerta Technology, UK. But, in case of pf-PANI, the measurements were restricted only up to  $70$  °C as the material becomes soft and starts to exhibit flow behavior thereafter. Heating beyond this temperature could damage the electrodes. The circular electrodes (dia = 33 mm) are of parallel plate type configuration and the samples used were about 0.4 mm thick. To ensure good electrical contact between the electrodes and the sample, the samples were coated with silver paste (about  $1.0$   $\mu\text{m}$ ) prior to measurements. The temperature dependence of the dielectric constant ( $\epsilon'$ ) and loss factor ( $\tan \delta$ ) of the blends were recorded. The relation between capacitance ( $C$ ) and the dielectric constant ( $\epsilon'$ ) given as  $\epsilon' = Ct/\epsilon_0 A$  is used to find the value of  $\epsilon'$ .<sup>32</sup> Here " $\epsilon_0$ " is the

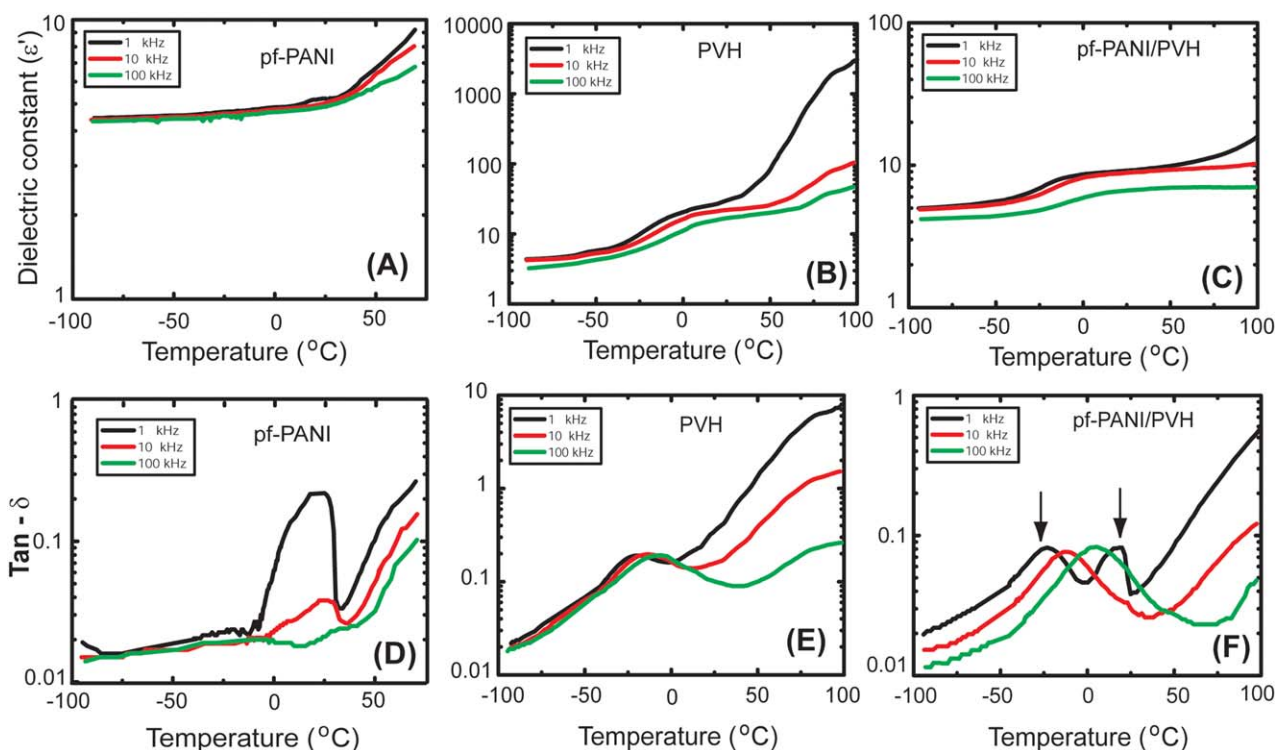


**Figure 1.** The variation of (A–C) dielectric constant as a function of temperature for pf-PANI, PVH and pf-PANI/PVH blend and (D–F) their corresponding  $\tan \delta$  variation as a function of temperature plotted at three different frequencies. [Color figure can be viewed in the online issue, which is available at wileyonlinelibrary.com.]

dielectric constant of free space ( $8.85 \times 10^{-12}$  F/m), “A” is the area of circular electrode, and “t” is the sample thickness.

**Conductivity Measurements.** The electrical conductivity ( $\sigma$ ) of the samples were found by measuring the change in resistance upon heating the sample at the heating rate of  $2^{\circ}\text{C}/\text{min}$  in a homemade glass chamber and using a Keithley 2002 multimeter. The  $\sigma$  is calculated using the formula  $\sigma = (1/R_b)(t/a)$  where “ $R_b$ ” is the bulk resistance of the sample and “a” is the sample area.<sup>33</sup> For electrical measurements, copper wires were connected on both the surfaces of the sample using silver paint and the sample was mounted on the sample holder, the temperature of which could be varied over the range RT to  $350^{\circ}\text{C}$ . The resistance measurements were made as a function of temperature by two terminal method and the real-time data were recorded using a Labview based computer controlled system.

**SEM Measurements.** The surface morphology of the blends was examined with a Carl Zeiss EVO 50 Scanning Electron Microscope with 10 kV operating voltage. The samples were sputter coated with gold on the viewing surface to enhance its conductivity.

## RESULTS AND DISCUSSION

### Dielectric and SEM Results

To understand the relaxation process in pf-PANI, PVH, and pf-PANI/PVH blend, as well as the influence of frequency on relaxation, the dielectric measurements were conducted at 1, 10, and 100 kHz and the variation of  $\epsilon'$  and  $\tan \delta$  as a function of temperature is displayed in Figure 1(A–F).

The pf-PANI exhibits a  $\epsilon'$  of about 4.5 and reveals only a slight increase in its value up to the measured temperature range ( $-100^{\circ}\text{C}$  to  $70^{\circ}\text{C}$ ) [see Figure 1(A)]. The pf-PANI, exhibits a relaxation between  $-10^{\circ}\text{C}$  and  $+30^{\circ}\text{C}$  at low frequency (1 kHz) and loses its signature at high frequency [100 kHz; see Figure 1(D)]. In a work on PANI doped with *para*-toluene sulfonic acid (p-TSA), a large change in  $\epsilon'$  from 1 kHz to 100 kHz (more than 1 order of magnitude) was observed and the change was attributed to interfacial polarization and movement of dipoles present in PANI.<sup>34</sup> Generally, interfacial polarization can be identified from its large change in dielectric constant with frequency (in kHz region) at room temperature.<sup>7,12</sup> In the present case, the  $\epsilon'$  of pf-PANI remains almost constant at all the three frequencies throughout the measured temperature range. Thus, the contribution from interfacial polarization is not that significant and hence the observed relaxation could be assigned as due to cumulative movement of dipoles present in pf-PANI chains.<sup>14,34</sup> In a multifrequency study on PANI doped with  $\beta$ -naphthalene sulfonic acid,<sup>35</sup> the authors have reported that the amplitude of the dielectric loss peak increases at low frequencies, which is in consonance with our results [see Figure 1(D)].

In case of PVH, the  $\epsilon'$  remains between 3 and 4 at very low temperatures. But, on passing about  $-40^{\circ}\text{C}$ , the  $\epsilon'$  starts to rise and reaches a value of more than 2 orders of magnitude at  $100^{\circ}\text{C}$  for low frequency [1 kHz; see Figure 1(B)]. The corresponding dielectric loss is also high [see Figure 1(E)]. The glass transition temperature ( $T_g$ ) of PVH is  $-33^{\circ}\text{C}$ .<sup>26,31</sup> Thus, this change is attributed to the dielectric relaxation of PVH on passing its  $T_g$ . Our recent free volume study on PVH reveals that

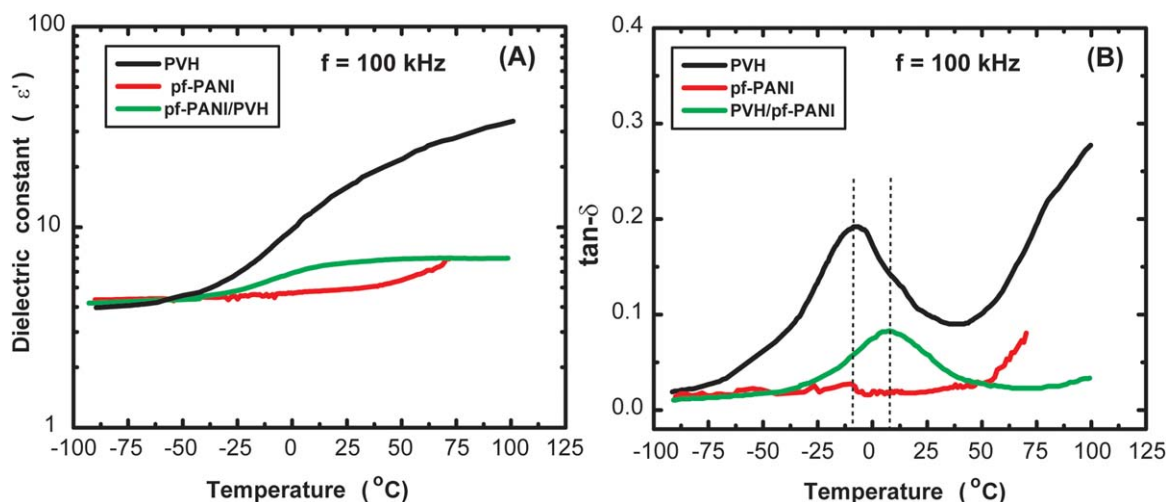


**Figure 2.** The variation of (A) dielectric constant ( $\epsilon'$ ) and (B)  $\tan \delta$  as a function of temperature for pf-PANI, PVH, and pf-PANI/PVH at 100 kHz. [Color figure can be viewed in the online issue, which is available at [wileyonlinelibrary.com](http://wileyonlinelibrary.com).]

the dielectric constant in PVH arises mainly due to dipole orientation polarization.<sup>26</sup> Below  $-40^{\circ}\text{C}$ , the PVH is in the glassy phase and hence the molecular motions are frozen in place due to which the dipoles cannot move to align themselves to the applied electric field. On passing  $T_g$ , the chain mobility of PVH increases owing to the availability of more free volume and polar groups start to move in response to the applied electric field, which increases the orientation of the molecules and the dielectric constant.<sup>26</sup> The  $\tan \delta$  peak associated with  $T_g$  shifts to high temperature with increase in frequency, inferring that the process is associated with dielectric relaxation.<sup>12</sup>

In case of pf-PANI/PVH blend, the  $\epsilon'$  exhibits only a slight rise throughout the temperature range studied for all the three frequencies, a feature which is close to that observed in case of pf-PANI. The  $\tan \delta$  shows two peaks at low frequency (1 kHz) one at about  $-30^{\circ}\text{C}$  which is due to  $T_g$  associated relaxation of PVH and the other one at about  $15^{\circ}\text{C}$  due to contribution from the dipoles of pf-PANI [see Figure 1(F)]. At high frequencies, the contribution from  $T_g$  of PVH is only evident as the pf-PANI relaxation becomes weak at high frequencies; a fact which is also clear from the frequency dependent plots of pf-PANI [see Figure 1(D)]. As mentioned earlier, if the  $\epsilon'$  arises due to interfacial polarization, then the  $\epsilon'$  exhibit an enormous decrease with increase in frequency (kHz region).<sup>3,7,8,12</sup> But, in the present pf-PANI/PVH system, there is no significant change in  $\epsilon'$  upon frequency change from 1 kHz to 100 kHz and the  $\tan \delta$  value remains minimum. Therefore, it can be concluded that interfacial polarization is not significantly contributing to the observed dielectric constant in this blend. This is in contradiction to the results reported for PANI/PVDF system where  $\epsilon'$  was reported to arise due to interfacial polarization.<sup>8</sup> This could be because PANI incorporated into PVDF acts just as a filler without any interaction, while pf-PANI interacts with PVH matrix through hydrogen bonding between C=O groups of pf-PANI and  $\text{CH}_2$  groups of PVH.<sup>31</sup>

Generally, when a miscible/partially miscible blend is formed and if the  $T_g$ s of the constituent polymers are far apart, it is

expected that the  $T_g$  of the resulting blend would shift towards each other.<sup>26,31,36</sup> The reported  $T_g$  of pf-PANI is about  $85^{\circ}\text{C}$ <sup>31</sup> and that of PVH is about  $-33^{\circ}\text{C}$ .<sup>26</sup> In order to understand the change in  $T_g$  upon blending, separate plots were made for  $\epsilon'$  and  $\tan \delta$  as a function of temperature at 100 kHz for pf-PANI, PVH, and pf-PANI/PVH blend [see Figure 2(A,B)].

At low temperatures, the value of  $\epsilon'$  for PVH, pf-PANI, and pf-PANI/PVH remains between 3 and 4, as seen earlier. In case of PVH, on passing a temperature of about  $-40^{\circ}\text{C}$ , the  $\epsilon'$  slowly rises and reaches a value of about 13 at  $100^{\circ}\text{C}$ . The dissipation factor ( $\tan \delta$ ) exhibits a clear relaxation with a peak at about  $-10^{\circ}\text{C}$ . The pf-PANI shows only a mild increase in  $\epsilon'$  and its  $\tan \delta$  value also start to slowly rise above  $40^{\circ}\text{C}$  due to increase in mobile charge carriers as it approaches its  $T_g$ . In case of pf-PANI/PVH blend, the  $\epsilon'$  value shows a little increase above  $-40^{\circ}\text{C}$  and settles to a value about 7 which is intermediate to the value for pf-PANI and PVH and is roughly half the value as compared with pure PVH. However, the  $\tan \delta$  peak shows an upshift with a peak value at about  $8^{\circ}\text{C}$ , but its peak height diminishes to less than half the value as compared with PVH. This shift in the peak value of  $\tan \delta$  of PVH by  $18^{\circ}\text{C}$  towards the  $T_g$  of pf-PANI confirms that this blend is partially miscible and supports our earlier results obtained by calorimetry and dynamic mechanical thermal analysis.<sup>31</sup>

As mentioned in the introduction, addition of 57 vol % of pf-PANI to PVH is a high filler content to reach the percolation threshold since generally 13 to 30 vol % is reported for PANI/PVDF-based PCD systems.<sup>8,9,12,29</sup> The constancy in  $\epsilon'$  for the blend even at high temperature with a value which is below that for PVH reveals that there is no percolation threshold-like effect. It is to be recalled here that the presence of conductive network near the percolation threshold in PVDF/PANI network has been reported to result in an abrupt increase in  $\tan \delta$  value by more than one order.<sup>6</sup> The constancy in  $\epsilon'$  together with low value of  $\tan \delta$  ( $\tan \delta < 0.1$ ) for the blend further suggests that there is no leakage current as there are no conductive network formation even at high temperatures [see Figure 2(B)].<sup>6,16</sup>



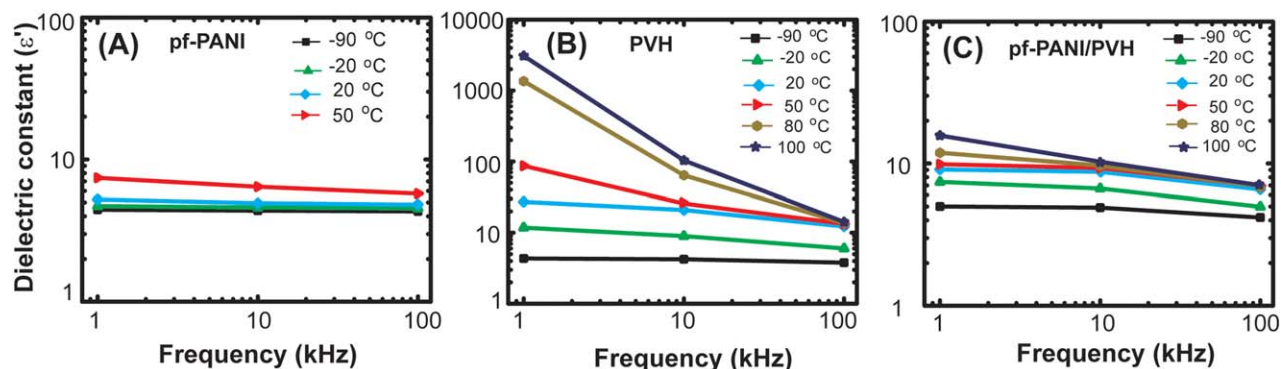


**Figure 3.** The variation of dielectric constant ( $\epsilon'$ ) as a function of frequency at selected temperatures for (A) pf-PANI, (B) PVH, and (C) pf-PANI/PVH. [Color figure can be viewed in the online issue, which is available at [wileyonlinelibrary.com](http://wileyonlinelibrary.com).]

The conductivity of pf-PANI is of the order of  $10^{-4}$  S/cm and the details regarding the conductivity will be discussed in the next section. For any system containing conducting component dispersed in an insulating polymer matrix, the capacitance is directly proportional to the cross-sectional area but inversely proportional to the thickness of the material.<sup>23</sup> Having understood that the interfacial polarization is not significantly contributing to the observed dielectric constant in this blend, we tried to correlate the results to microcapacitance structure model.<sup>13,14</sup> According to this model, the addition of conductive fillers to an insulation matrix would generate numerous microcapacitors. Here, the conducting pf-PANI particles present in the PVH matrix is expected to act as minute capacitor and increase the value of dielectric constant. Upon pf-PANI/PVH blend formation, the less polar  $\alpha$ -PVDF of PVH gets modified to  $\beta$ -form which is more polar.<sup>31</sup> Thus, one expects higher dielectric constant in the blend as compared with PVH. As discussed earlier, even after addition of 57 vol % of pf-PANI to PVH, the  $\epsilon'$  value remained lower than that of the base polymer PVH, which is surprising [see Figure 2(A)]. This behaviour in pf-PANI/PVH blend is similar to that observed in PANI nano-flakes coated on graphene and blended with PVDF system.<sup>4</sup>

This low value of  $\epsilon'$  for the blend could be due to hydrogen bonding interaction between pf-PANI and PVH matrix.<sup>31</sup> On account of this interaction, the polar groups in PVH are not able to orient freely in spite of the increased free volume available at high temperatures. It is possible that the hydrogen bonding interaction suppresses the ability of PVH dipoles that can orient to the applied electric field and hence the effective dielectric constant remains lower than that of PVH. It is also known that increased cross-linking in PANI chains through the formation of interchain bonds restrict the main chain motion and decrease the  $\epsilon'$  value,<sup>34</sup> which is in consonance with our results. Thus, in the present case, the decrease in  $\epsilon'$  value of the blend could also be associated with the decrease in main chain motion of pf-PANI upon hydrogen bond formation.

The change in dielectric constant as a function of frequency is shown at selected temperatures [Figure 3(A–C)]. In all these cases, the values of  $\epsilon'$  and  $\tan \delta$  decreases with increase in frequency as observed in other PANI/polymer blends.<sup>12,20–22</sup> It is obvious from Figure 3(A–C) that the dielectric constant increases with increase

in temperature. The increase is more in the low frequency region (1 kHz) as compared with high frequency region (100 kHz). The combined influence of frequency and temperature on the  $\epsilon'$  can be explained as follows. At low frequencies, the dipoles and charge carriers had sufficient time to orient in the direction of the applied electric field and contribute to increase in  $\epsilon'$  value.<sup>33</sup> At high temperatures, the increased availability of free volume facilitates the orientation of dipoles of a polar polymer and results to increase in dielectric constant, as discussed earlier. Thus, we can conclude that these samples exhibit maximum dielectric constant at low frequencies and high temperatures.

In summary, from the dielectric measurements, it can be concluded that there is no significant contribution towards  $\epsilon'$  for this blend from interfacial polarization. The hydrogen bonding interaction between pf-PANI and PVH do not allow the dipoles of PVH to orient to the applied field as well as restrict the main chain mobility of pf-PANI. Thus, the blend has lower  $\epsilon'$  as compared with PVH.

The SEM morphology of the blend sample obtained at room temperature and the sample that was quench cooled from 120 °C gives further evidence for the absence of conductive networks in the blend [Figure 4(A,B)]. The SEM pictures of the blend obtained at room temperature showed a clear uniform distribution of pf-PANI particles with size about 620 nm.<sup>31</sup> Almost similar morphological features were observed for the sample heated up to 120 °C with slightly distorted particle shape and with no connectivity between the particles [Figure 4(A,B)].<sup>37</sup> This could be because of the almost similar thermal expansion coefficient of pf-PANI and PVH matrices, which ensures that the effective gaps remain unchanged as the temperature increases. Thus, the percolation threshold-like effect is not seen and the value of  $\epsilon'$  remains low for the blend even at high temperatures. It is possible that the two pyrene groups attached to the PANI backbone through the alkyl tails in pf-PANI restrict the close association of pf-PANI chains and formation of a conductive network. The schematic diagram of pf-PANI/PVH blend with pf-PANI content of 57 vol % ( $f_{\text{pf-PANI}} = 0.57$ ) depicting the hindrance towards forming a continuous network of pf-PANI particles is shown in Figure 4(C).

Now, we will use some theoretical models and validate the obtained dielectric results for pf-PANI/PVH blend.<sup>18</sup> The plot depicting the theoretical models together with experimental

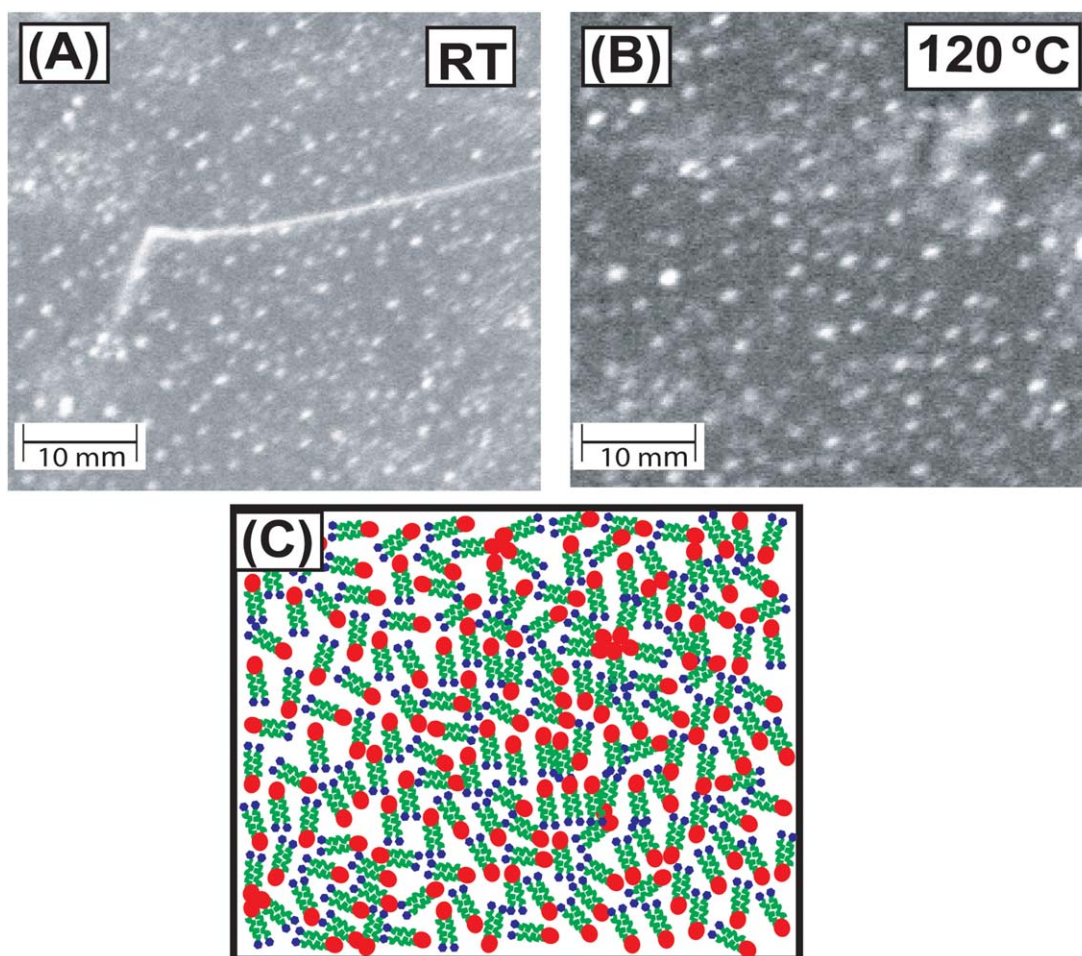


**Figure 4.** The SEM images showing the surface morphology of pf-PANI/PVH blend at (A) room temperature, (B) sample quench cooled from 120 °C, and (C) schematic illustration showing hindrance to achieve interconnected network in pf-PANI/PVH blend. [Color figure can be viewed in the online issue, which is available at [wileyonlinelibrary.com](http://wileyonlinelibrary.com).]

values for the dielectric constant of this blend measured at room temperature for frequencies 1, 10, and 100 kHz are shown in Figure 5.

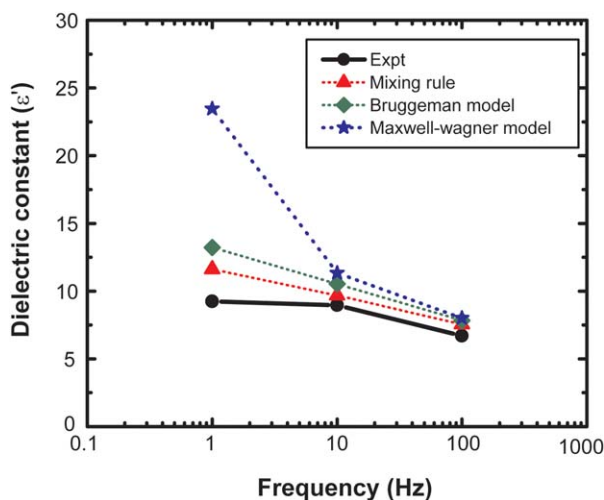


**Figure 5.** Theoretical and experimental plots of dielectric constant for pf-PANI/PVH blend at three different frequencies. [Color figure can be viewed in the online issue, which is available at [wileyonlinelibrary.com](http://wileyonlinelibrary.com).]

**Logarithmic Mixing Rule.** Using logarithmic mixing rule, it is possible to estimate the dielectric constants of the PCD system, if the  $\epsilon'$  of the base polymer and filler are known and is applicable to systems where the dielectric constant of the polymer matrix differs slightly from that of the filler.<sup>38</sup> This rule is given as,

$$\log \epsilon_c = v_m \log \epsilon_m + v_f \log \epsilon_f \quad (1)$$

where  $\epsilon_c$  is the dielectric constant of the resultant polymer composite;  $\epsilon_m$  is the dielectric constant of the polymer matrix; and  $\epsilon_f$  is the dielectric constant of the filler particles.<sup>18</sup> Here  $v_m$  and  $v_f$  are the volume fraction of polymer matrix (PVH;  $v_m = 0.43$ ) and filler (pf-PANI;  $v_f = 0.57$ ), respectively. The theoretical values were slightly higher as compared with experimental results at high frequencies while the deviation between them increases with decrease in frequency (see Figure 5).<sup>18</sup>

**Bruggeman Model.** The Bruggeman model is used to predict the dielectric constant of the composite system at high volume fraction of filler.<sup>39</sup> This model is developed on the basis of percolation theory and dipole-dipole interaction among the filler particles. Using this model, one can predict the dielectric constant of the PCD system as

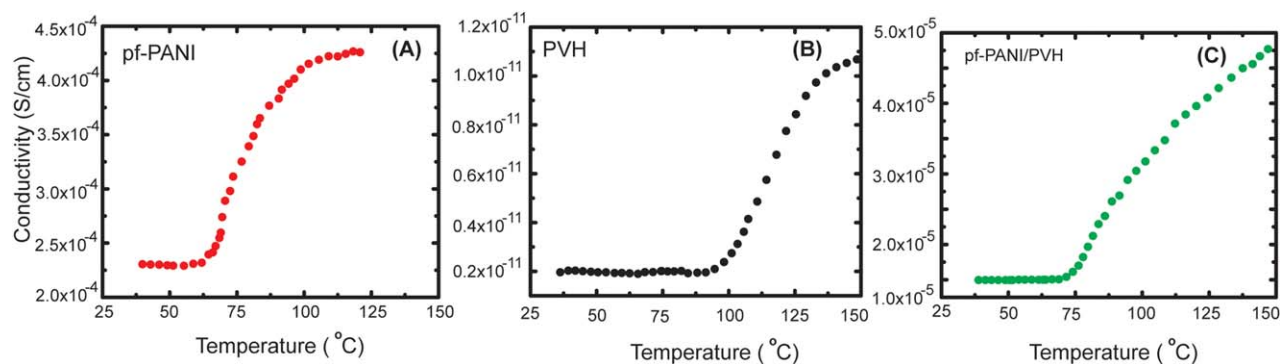


**Figure 6.** Variation of conductivity ( $\sigma$ ) as a function of temperature for pf-PANI, PVH, and pf-PANI/PVH blend. [Color figure can be viewed in the online issue, which is available at [wileyonlinelibrary.com](http://wileyonlinelibrary.com).]

$$\varepsilon_c = \left\{ H + [H^2 + 8 \varepsilon_f \varepsilon_m]^{1/2} \right\} / 4$$

where,  $H = (3\nu_f - 1)\varepsilon_f + (2 - 3\nu_f) \varepsilon_m$

Similar to previous case, the predicted theoretical value slightly deviates from experimental values at high frequency (100 kHz) while more deviation is observed at low frequency (1 kHz). The deviation could be due to nonaccountability of this model towards the interphase interaction generated between the polymer matrix and the filler inclusions.<sup>18</sup>

**Maxwell-Wagner Model.** This model mainly deals with the effect of interfacial polarization.<sup>38</sup> Similar to first case, this model is applicable to predict the dielectric constant of the composite systems when the difference in permittivity between the polymer and the filler is not large. The equation based of Maxwell-Wagner model is given as<sup>18,38</sup>

$$\varepsilon_c = \varepsilon_m [2\varepsilon_m + \varepsilon_f + 2\nu_f (\varepsilon_f - \varepsilon_m)] / [2\varepsilon_m + \varepsilon_f - \nu_f (\varepsilon_f - \varepsilon_m)]$$

This model also does not take into account of the interphase interaction between the polymer and the filler particles.<sup>18</sup>

In a recent report on PANI/EVA composite system, the authors have obtained the experimental values higher as compared with model predictions.<sup>18</sup> Interestingly, in the present pf-PANI/PVH system, the experimental values are lower as compared with model predictions. This could be because pf-PANI interacts with PVH matrix through hydrogen bonding leading to a partial miscible blend, thus lowering the interfaces while in PANI/EVA system, PANI acts just as fillers in EVA matrix without any interaction.

### Conductivity Results

The variation of conductivity ( $\sigma$ ) as a function of temperature for pf-PANI, PVH, and pf-PANI/PVH are shown in Figure 6(A–C). The room temperature conductivity for pf-PANI, PVH, and pf-PANI/PVH are  $2.2 \times 10^{-4}$  S/cm,  $2.0 \times 10^{-12}$  S/cm, and  $1.0 \times 10^{-5}$  S/cm. The dielectric and conducting properties of PANI crucially depend on the degree of doping, test frequency, and test temperature.<sup>34</sup> In case of PANI, the conductivity can be tuned by acid doping from  $10^{-10}$  S/cm up to 100 S/cm.<sup>40</sup> The electronic conductivity of doped PANI is always associated with the protonation of PANI and thus depends on the degree of protonation.<sup>41</sup> The protons because of their high mobility are the dominating charge carriers in PANI doped with strong

acids.<sup>41</sup> Thus, the protons are free to move over a long distance along a chain and can hop among different chains.

The obtained conductivity of pf-PANI lies between that of PANI which is in completely protonated form ( $10^{-2}$  to  $10^{-3}$  S/cm)<sup>21,28</sup> and fully reduced form ( $10^{-10}$  to  $10^{-7}$  S/cm).<sup>40</sup> This result is in accordance with the fact that pf-PANI is partially protonated as can be seen from its structure (see Scheme 1). The conductivity value of PVH is close to its reported value.<sup>14</sup>

In case of PANI/PVDF blend, a conductivity of  $1.8 \times 10^{-7}$  S/cm has been reported when the PANI content is <5% and was proposed as a semiconductor film to serve as energy storage material.<sup>6</sup> The pf-PANI/PVH blend yielded conductivity higher by 2 orders as compared with PANI/PVDF blend. In these films, conduction is influenced by tunneling effect which results only in a minimal leakage current because of the existence of PVH insulation layers which serves as electrical barriers to impair direct contacts between pf-PANI particles. Very recently, it has been reported that PVH upon 30% incorporation of PANI (doped with DBSA) resulted to conductivity which is lower by 3 orders compared with our results.<sup>14</sup> This difference could be attributable to the type and the amount of acid used for doping PANI.

Upon heating, the conductivity of pf-PANI starts to increase gradually at about 60°C to reach a value of  $4.2 \times 10^{-4}$  S/cm at about 100°C and almost saturates thereafter since pf-PANI starts to flow. In case of PVH, the conductivity starts to increase at about 100°C to reach a value of  $1.0 \times 10^{-10}$  S/cm at 150°C. For the blend, the conductivity starts to increase at about 75°C, rises steadily up to 150°C to reach a value of  $4.5 \times 10^{-5}$  S/cm [Figure 6(C)]. Please note that in case of blend, the conductivity starts to increase at a temperature which is intermediate to that of pf-PANI and PVH.

From the dielectric results, it is clear that pf-PANI particles do not exhibit any connectivity even after heating the blend up to 100°C. The SEM picture further confirms this aspect. As the protons are the main charges for conductivity in PANI, the factors that affect the long range mobility of PANI will also affect its conductivity  $\sigma$ .<sup>34</sup> Since the pf-PANI particles in this blend are hydrogen bonded to PVH chains, as stated earlier, it is possible that the flexibility of pf-PANI chains get reduced which in turn can influence its conductivity ( $\sigma$ ). Furthermore, the pyrene moieties together with alkyl tails could restrict the close



association of pf-PANI [see schematic picture Figure 4(C)] and thereby restrict the hopping of charge carriers and  $\sigma$ .<sup>31</sup> Thus, the slow and steady rise in  $\sigma$  value for the blend is in agreement with the dielectric measurement results not showing percolation threshold-like change and SEM not revealing interconnected network. If there had been a direct contact between the particles forming a continuous path, then the conductivity would have increased by 2 orders of magnitude.<sup>6</sup> Thus, we propose that the observed steady increase in conductivity as shown in Figure 6, is due to mobility/hopping of charge carriers and not due to interconnectivity of pf-PANI particles.

Previous experiments have shown that temperature can influence the percolation threshold in PVDF based composites. In case of Ni-PVDF composite, upon heating above percolation threshold, metal-insulator transition has been observed because of which the conductivity of Ni-PVDF composite decreased from  $10^{-4}$  to  $10^{-6}$  S/cm and the  $\epsilon'$  value also dropped upon heating.<sup>3</sup> With the increase in temperature, the thermal expansion of PVDF interrupted the conducting path of the percolating Ni clusters due to difference in thermal expansion coefficient and this has led to the observed metal-insulator transition with temperature.<sup>3</sup>

Based on the discussions made above, it is clear that in pf-PANI/PVH blend, it is not possible for the pf-PANI particles to form a conductive network in PVH matrix. Also, in the temperature range studied, the dielectric constant of the blend increases from 4 to 15 and the  $\tan \delta$  value remains much below 1.0 (at 1 kHz) not showing any leakage current [see Figure 1(C,F)]. All these results reveal that the pf-PANI in the PVH matrix has not formed any conductive network even at a high temperature of 100 °C and is in consonance with SEM findings. This could be due to the bulky pyrene groups attached through the alkyl tails to PANI backbone in pf-PANI not permitting the pf-PANI particles to associate and to form a conductive network which could have led to significant enhancement in conductivity [see schematic diagram; Figure 4(C)]. Thus, in the present case, even with  $f_{\text{pf-PANI}} = 0.57$ , which is much higher than the volume fraction of fillers reported for PANI/PVDF-based systems showing percolation threshold,<sup>8,9,12,29</sup> we did not find any evidence for the presence of connective networks that could lead to leakage current despite of the reasonably good conductivity exhibited by pf-PANI.

Now, let us try to understand the relationship between  $\epsilon'$  and  $\sigma$ . As seen from the thermal behavior of pf-PANI, PVH, and pf-PANI/PVH, both  $\epsilon'$  and  $\sigma$  increases as a function of temperature. In case of solid polymer electrolytes, it is known that increase in  $\epsilon'$  generally leads to increase in  $\sigma$  which is due to either increase in charge mobility and/or concentration of charge carriers.<sup>42</sup> In case of polar polymers such as PVH and pf-PANI, the  $\epsilon'$  increases with increase in temperature due to the availability of more free volume and easy orientation of the dipoles.<sup>26,43</sup> The ease of polymer chain movements at high temperatures also enables enhanced hopping of mobile charges and thus  $\sigma$  also increases steadily with temperature.<sup>33</sup> Thus, increase in  $\epsilon'$  results to increase in  $\sigma$ .

The existence of PVH insulation layers that serve as electrical barriers between neighboring pf-PANI particles as well as the bulky pyrene groups attached to PANI backbone through alkyl tails in pf-PANI seems to impair the formation of leakage current, store charges as microcapacitor and lead to almost constant value of dielectric permittivity of pf-PANI/PVH blend. The conductivity also increases gradually with temperature and does not increase several order of magnitudes like that in an insulating-conducting transition also goes in agreement with the prediction of microcapacitor structure reported.<sup>6</sup> A thorough study on the addition of pf-PANI in different molar ratios to PVH is on progress to understand the influence of the extent of hydrogen bonding on the size and distribution of pf-PANI in PVH matrix.

## CONCLUSIONS

The results reveal that interfacial polarization do not govern the dielectric response of pf-PANI/PVH composite and the plausible origin of dielectric constant is due to the formation of microcapacitors. The SEM image of the heated blend did not reveal any interconnected particles that could lead to conductivity, which is in agreement with conductivity results and supports the microcapacitor structure model. The study also reveals that there is hindrance to achieve percolation threshold in pf-PANI/PVH system even after addition of 57 vol % of pf-PANI.

## ACKNOWLEDGMENTS

The authors thank Director, DMSRDE, Kanpur, for the encouragement, support, and for giving permission to publish this work. The authors also thank Ms. Kavitha Agarwal of DMSRDE for her help in SEM characterization. One of the authors (V.P.S.), gratefully acknowledges DRDO for the financial assistance in the form of a Research Associateship.

## REFERENCES

1. Nalwa, H. S. Eds. *Ferroelectric Polymers. Chemistry, Physics and Applications*; Marcel Dekker: New York, **1995**.
2. Zhang, Q. M.; Li, H.; Poh, M.; Xia, F.; Cheng, Z. Y.; Xu, H.; Huang, C. *Nature* **2002**, *419*, 284.
3. Dang, Z. M.; Lin, Y. H.; Nan, C. W. *Adv. Mater.* **2003**, *15*, 1625.
4. Shang, J.; Zhang, Y.; Yu, L.; Luan, X.; Shen, B.; Zhang, Z.; Lv, F.; Chu, P. K. *J. Mater. Chem. A* **2013**, *1*, 884.
5. Qi, L.; Lee, B. I.; Chen, S.; Samuels, W. D.; Exarhos, G. J. *Adv. Mater.* **2005**, *17*, 1777.
6. Yuan, J. K.; Dang, Z. M.; Yao, S. H.; Zha, J. W.; Zhou, T.; Li, S. T.; Bai, J. *J. Mater. Chem.* **2010**, *20*, 2441.
7. Zhu, J.; Shen, J.; Guo, S.; Sue, H. *J. Carbon* **2015**, *84*, 355.
8. Li, L.; Zhang, B. Q.; Chen, X. M. *Appl. Phys. Lett.* **2013**, *103*, 192902.
9. Huang, C.; Zhang, Q. *Adv. Funct. Mater.* **2004**, *14*, 501.
10. Pud, A.; Ogurtsov, N.; Korzhenko, A.; Shapoval, G. *Prog. Polym. Sci.* **2003**, *28*, 1701.



11. Bliznyuk, V. N.; Baig, A.; Singamaneni, S.; Pud, A. A.; Fatyeyeva, K. Y.; Shapoval, G. S. *Polymer* **2005**, *46*, 11728.
12. Bobnar, V.; Levstik, A.; Huang, C.; Zhang, Q. M. *J. Non-Cryst. Solids* **2007**, *353*, 205.
13. He, F.; Lau, S.; Chan, H. L.; Fan, J. *Adv. Mater.* **2009**, *21*, 710.
14. Soares, B. G.; Pontes, K.; Marins, J. A.; Calheiros, L. F.; Livi, S.; Barra, G. M. O. *Eur. Polym. J.* **2015**, *73*, 65.
15. Yang, W.; Yu, S.; Sun, R.; Ke, S.; Huang, H.; Du, R. *J. Phys. D: Appl. Phys.* **2011**, *44*, 475305.
16. Yuan, J. K.; Dang, Z. M.; Bai, J. *Phys. Stat. Sol. RRL* **2008**, *2*, 233.
17. Pant, H. C.; Patra, M. K.; Negi, S. C.; Bhatia, A.; Vadera, S. R.; Kumar, N. *Bull. Mater. Sci.* **2006**, *29*, 379.
18. Rahaman, M.; Chaki, T. K.; Khastgir, D. *Eur. Polym. J.* **2012**, *48*, 1241.
19. Banerjee, P.; Mandal, B. M. *Macromolecules* **1995**, *28*, 3940.
20. Dutta, P.; Biswas, S.; De, S. K. *Mater. Res. Bull.* **2002**, *37*, 193.
21. Chwang, C. P.; Liu, C. D.; Huang, S. W.; Chao, D. Y.; Lee, S. N. *Synth. Met.* **2004**, *142*, 275.
22. Lu, J.; Moon, K. S.; Kim, B. K.; Wong, C. P. *Polymer* **2007**, *48*, 1510.
23. Rahaman, M.; Chaki, T. K.; Khastgir, D. *Polym. Eng. Sci.* **2014**, *54*, 1632.
24. Zhang, Q. M.; Bharti, V.; Zhao, X. *Science* **1998**, *280*, 2101.
25. Martins, P.; Lopes, A. C.; Lanceros-Mendez, S. *Prog. Polym. Sci.* **2014**, *39*, 683.
26. Ramani, R.; Das, V.; Singh, A.; Ramachandran, R.; Amarendra, G.; Alam, S. *J. Phys. Chem. B* **2014**, *118*, 12282.
27. Huang, C.; Zhang, Q. M.; Su, J. *Appl. Phys. Lett.* **2003**, *82*, 3502.
28. Yu, L.; Zhang, Y.; Tong, W.; Shang, J.; Lv, F.; Chu, P. K.; Guo, W. *Compos. A* **2012**, *43*, 2039.
29. Derouiche, H.; Mohamed, A. B. *Thin Solid Films* **2012**, *526*, 274.
30. Martins, J. N.; Kersch, M.; Altstädt, V.; Oliveira, R. V. B. *Polym. Test.* **2013**, *32*, 862.
31. Singh, V. P.; Ramani, R.; Pal, V.; Prakash, A.; Alam, S. *J. Appl. Polym. Sci.* **2014**, *131*, 40163.
32. Dang, Z. M.; Yao, S. H.; Yuan, J. K.; Bai, J. *J. Phys. Chem. C* **2010**, *114*, 13204.
33. Aziz, S. B.; Abidin, Z. H. Z. *J. Appl. Polym. Sci.* **2015**, *132*, DOI: 10.1002/app.41774.
34. Bhadra, S.; Singha, N. K.; Khastgir, D. *Polym. Int.* **2007**, *56*, 919.
35. Dutta, P.; Biswas, S.; De, S. K. *J. Phys.: Condens. Mater.* **2001**, *13*, 9187.
36. Wästlund, C.; Berndtsson, H.; Maurer, F. H. J. *Macromolecules* **1998**, *31*, 3322.
37. Wu, C.; Huang, X.; Wu, X.; Yu, J.; Xie, L.; Jiang, P. *Compos. Sci. Technol.* **2012**, *72*, 521.
38. Cho, S. D.; Lee, S. Y.; Hyun, J. G.; Paik, K. W. *J. Mater. Sci. Mater. Electron* **2005**, *16*, 77.
39. Vo, H. T.; Shi, F. G. *Microelectron. J.* **2002**, *33*, 409.
40. Pinto, N. J.; Acosta, A. A.; Sinha, G. P.; Aliev, F. M. *Synth. Met.* **2000**, *113*, 77.
41. Stejskal, J.; Bogomolova, O. E.; Blinova, N. V.; Trchová, M.; Šeděnková, I.; Prokeš, J.; Sapurina, I. *Polym. Int.* **2009**, *58*, 872.
42. Aziz, S. B.; Abidin, Z. H. Z. *Mater. Chem. Phys.* **2014**, *144*, 280.
43. Aziz, S. B. *Iran Polym. J.* **2013**, *22*, 877.